UNITED NATIONS UNIVERSITY
UNU-GTP
Geothermal Training Programme

Orkustofnun, Grensasvegi 9,
IS-108 Reykjavik, Iceland

40th Anniversary Workshop
April 26 2018

WELLBORE STABILITY ANALYSIS IN GEOTHERMAL WELL DRILLING

Samuel Ikinya Nganga
Kenya Electricity Generating Company, Ltd. – KenGen
P.O. Box 785-20117
Naivasha
KENYA
snganga@kengen.co.ke

ABSTRACT

Drilling progress is affected by various downhole challenges encountered during drilling that impact on wellbore stability. The main challenges are loss of circulation and borehole wall collapse that lead to stuck drilling string, problems in landing casings and liners and in extreme cases loss of drill string components and abandonment of the well. Wellbore instabilities encountered during drilling can add to the overall cost of a geothermal well by consumption of more materials and extension of well completion time. Minimum stress σ_3 (fracture pressure) from Eaton´s formula and overburden stress σ_1 form the maximum and minimum principal field stresses in normal faulting systems such as Olkaria in the Kenyan rift. These stresses are used to calculate effective hoop, radial and vertical stresses at the wellbore wall that control borehole failure if the formation strength is exceeded. Maximum compressive hoop stress occurs at 90° and 270° and minimum hoop stress at 0° and 180° in vertical well indicating the direction of minimum and maximum horizontal stresses, respectively. In directional wells the hoop stresses are dependent on the well inclination and azimuth. Radial stress emanates from drilling fluid pressure and varies with variation in fluid density. Variation of stresses around wellbore wall are demonstrated using vertical and directional wells at OW-731 in Olkaria geothermal field Kenya by developing Mohr's circles at different drilling fluid densities.

1. INTRODUCTION

Olkaria geothermal field is located within a volcanic complex in southern part of the Kenyan East African Rift System (Munyiri, 2016). The field is classified as high-enthalpy geothermal field with temperatures above 200°C within 1000 m depth and is currently supporting over 650 MW of electricity generation (Ouma et al., 2016). Well drilling represents a significant portion of geothermal development cost and accounts for 30-50% of the total cost of a geothermal plant (Finger and Blankenship, 2010; European Union, 2015). Improvement of drilling practices and methods have the potential of lowering the well cost. Similarly, analysis of challenges encountered during actual drilling operation and their solutions have an impact in well delivery in time and cost.

Well drilling upsets the formation balance that exists before formation removal through the action of the drill bit. Drilling fluids either mud, air, aerated mud or foam assists in wellbore support as well as in removal of cuttings generated at well bottom. Maintaining the correct flowrates of the drilling fluids impacts the wellbore stability and lower the chances of formation damages during drilling (Mitchell and Miska, 2011; Zoback, 2010). According to the African Union Code of Practice for Geothermal Drilling

(African Union, 2016), information on the expected well path sub-surface conditions is important in planning for well instability challenges. In addition to pressure, temperature and reservoir fluid properties, the relevant geological information should be assessed (African Union, 2016). Well instability can be grouped into two categories namely mechanical related instability and physical-chemical. Mechanical related instability refers to the situation when there is collapse or failure in the wellbore due to stresses, erosion, pressures (surge and swab) and drill string action. Physical-chemical instability involves interactions between drilling fluids and formation that result in swelling or dispersion of the formation (Fjær et al., 2008).

Cases of wellbore instability are associated with stuck drill string, loss of circulation (LOC) tight spots, caving, wellbore collapse and sidetracking. These conditions result in increased cost and NPT of drilling operations. Wellbore instabilities such as loss of drilling fluid circulation and wellbore collapse requires measures to counter during drilling and can lead to extra operations such as fishing to remove drilling tools, cementing to stabilize collapsing formations, side tracking to change the well course and in extreme cases instability can result in total abandonment of the well (Azar and Samuel, 2007; Finger and Blankenship, 2010).

2. WELLBORE STRESSES

Drilling removes natural materials thereby altering formation strength and introduces fluids into the formation. This can initiate failure depending on the mechanical properties of the rock (Economides et al., 1998). Around the wellbore is a stress concentration field and the forces acting within the well profile from the drilling fluids and formation pressure can result in well collapse and other problems. Wellbore failure occurs when the stress concentrated around the circumference of the well exceeds the formation strength. Knowledge of stress magnitude and direction in a well helps in solving problems associated with wellbore instabilities, regulating drilling fluid density, casing setting point, cementing, drill bit and other important parameters of well drilling operation (Zoback, 2010; Zoback, et al., 2003).

2.1 Stress and principal stresses

Well drilling activities involve loading and unloading cycles and the stress-strain relationship demonstrates the material response to applied loads (Economides et al., 1998). Stress is force acting over an area and describes the density of forces passing through a given point. It can be resolved into normal stress σ, perpendicular to the surface, and shear stress τ, acting along the plane. In three-dimensions, stress is a tensor quantity and is expressed in six independent components (Harrison and Hudson, 2000). Principal stresses are resultant normal stresses in three perpendicular planes in which the shear stress components reduce to zero. The three perpendicular planes define the principal axes of the stress with only normal stresses as shown in Equation 1 (Kearey et al., 2002):

$$\sigma_{ij} = \begin{bmatrix} \sigma_{xx} & \tau_{xy} & \tau_{xz} \\ \tau_{xy} & \sigma_{yy} & \tau_{yz} \\ \tau_{xz} & \tau_{yz} & \sigma_{zz} \end{bmatrix} = \begin{bmatrix} \sigma_{xx} & 0 & 0 \\ 0 & \sigma_{yy} & 0 \\ 0 & 0 & \sigma_{zz} \end{bmatrix} \quad (1)$$

Principal stresses represent the maximum, intermediate and minimum stresses denoted by σ_1, σ_2, and σ_3 and are perpendicular to each other (Fjær et al., 2008). For any induced stress state in rock formation such as in drilling, the maximum and minimum normal stresses occur on the principal stress planes oriented parallel and perpendicular to the wellbore wall (Harrison and Hudson, 2000). One principal stress pre-existing in a field (in situ) is generally normal to the Earth's surface with the other two principal stresses acting in an approximately horizontal plane. To analyze state of stress at depth, field principal stress magnitudes S_v, the vertical stress; S_{Hmax}, the maximum principal horizontal stress and S_{hmin}, the minimum principal horizontal stress are considered depending on the faulting system existing in the field summarized in Table 1 (Zoback, 2010).

TABLE 1: Faulting system and associated stresses (Zoback, 2010)

Faulting system	Stress		
	σ_1	σ_2	σ_3
Normal	S_v	S_{Hmax}	S_{hmin}
Reverse	S_{Hmax}	S_{hmin}	S_v
Strike-slip	S_{Hmax}	S_v	S_{hmin}

Pore pressure (P_p) acts on the fluids in the pore spaces of the rock. It is related to the hydrostatic pressure (P_f) and increases with depth in normal conditions. Hydrostatic pressure is the pressure exerted by a column of fluid expressed in Equation 2 (Rabia, 2001).

$$P_f = \rho g h \tag{2}$$

2.2 Stress around the wellbore

Wellbore creates a new rock surface and new stress field that concentrates stress around the wellbore wall. The principal stresses in the rock mass then align perpendicular and parallel to the borehole wall. If the concentrated stress exceeds the formation strength, failure will occur. The magnitude of the stress and the formation properties determine the nature of failure that can occur in the well (Aadnoy and Looyeh, 2011).

In a vertical well, the vertical principal stress is parallel to the wellbore axis. Horizontal principal stresses are perpendicular to the wellbore and converge in the direction of minimum horizontal stress S_{hmin} direction increasing compressive stress. In the direction of maximum horizontal stress S_{Hmax}, the stresses diverge decreasing compressive stress. Increased compressive stresses can result in borehole breakouts if the shear strength at the borehole wall exceeds the rock's shear strength. Decreased compressive stresses induces tensile stress that can result in tensile failure (fracture) of the borehole wall (Zoback, 2010). Effective principal stresses around vertical borehole wall are hoop, radial and vertical expressed in Equations 3 – 5 (Zoback, 2010):

$$\sigma_{\theta\theta} = \sigma_{hmin} + \sigma_{Hmax} - 2(\sigma_{Hmax} - \sigma_{hmin})cos2\theta - 2P_p - \left(P_f - P_p\right) - \sigma^{\Delta T} \tag{3}$$

$$\sigma_{rr} = \left(P_f - P_p\right) = \Delta P \tag{4}$$

$$\sigma_{zz} = \sigma_v - 2\vartheta(\sigma_{Hmax} - \sigma_{hmin})cos2\theta - P_p - \sigma^{\Delta T} \tag{5}$$

where σ_{Hmax} = maximum horizontal stress;
σ_{hmin} = minimum horizontal stress;
σ_v = vertical stress;
ϑ = Poison's ratio;
θ = angle measured clockwise from the direction of σ_{Hmax};
$\sigma_{\theta\theta}$ is the Hoop Stress; and
σ_{rr} is the radial stress;
Stress $\sigma^{\Delta T}$ is the thermal stress induced by temperature difference;
P_f is drilling fluid pressure; and
P_p is the pore pressure.

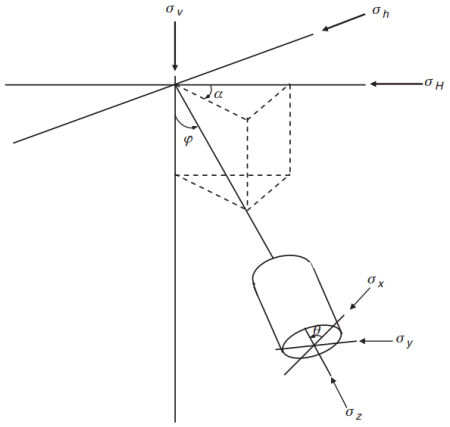

FIGURE 1: Stresses on wellbore wall in a directionally drilled well (Mitchell & Miska, 2011)

In a directionally drilled well, the field principal stresses are not aligned to the well axis but are dependent on the orientation of the well in relation to the existing field stress magnitude and direction. The stresses must be transformed to the well orientation with respect to the in-situ stresses, well inclination and azimuth as shown in Figure 1 (Zoback, 2010; Mitchell and Miska, 2011). The transformed stresses are then converted into three normal σ_{rr} $\sigma_{\theta\theta}$ and σ_{zz} and three shear stresses $\tau_{r\theta}$, τ_{rz} and $\tau_{\theta z}$ based on

angle θ around the borehole wall which are then used to calculate principal effective stresses. The resultant stresses are radial stress σ_{rr} acting normal to the wall and two tangential (hoop) stresses σ_{tmax} and σ_{tmin} expressed in Equations 6-8 (Renpu, 2011; Zoback, 2010; Mitchell and Miska, 2011):

$$\sigma_r = \Delta P = (P_f - P_p) \tag{6}$$

$$\sigma_{\theta max} = \frac{1}{2}\left(\sigma_{zz} + \sigma_{\theta\theta} + \sqrt{(\sigma_{zz} - \sigma_{\theta\theta})^2 + 4\tau_{\theta z}^2}\right) \tag{7}$$

$$\sigma_{\theta min} = \frac{1}{2}\left(\sigma_{zz} + \sigma_{\theta\theta} - \sqrt{(\sigma_{zz} - \sigma_{\theta\theta})^2 + 4\tau_{\theta z}^2}\right) \tag{8}$$

2.3 Mohr-Coulomb failure criterion

Stress state at a point can be presented graphically using Mohr's Circle drawn in the normal and shear stress plane. In the principal coordinate system, shear stresses reduce to zero and normal stresses are the maximum and minimum principal stresses. Normal and shear stresses are expressed in Equations 9 and 10 (Jaeger et al., 2007):

$$\sigma = \frac{\sigma_1 + \sigma_3}{2} + \frac{\sigma_1 - \sigma_3}{2} cos2\theta \tag{9}$$

$$\tau = \frac{\sigma_1 - \sigma_3}{2} sin2\theta \tag{10}$$

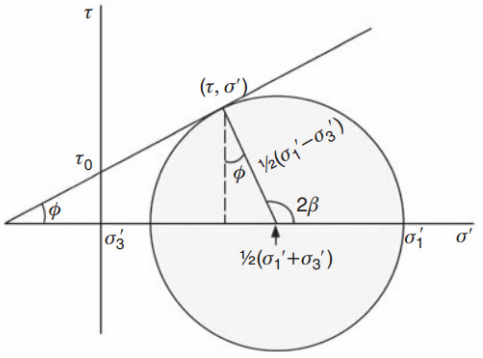

Figure 1: Mohr-Coulomb Failure Criterion (Mitchell and Miska, 2011)

Plotting shear stress against normal stress traces a stress envelop circle referred to as a Mohr's circle. A line tangent to the circle given by Equation 11 defines the Mohr-Coulomb failure criterion (Azar and Samuel, 2007).

$$\tau = \pm(C + \sigma'_n tan\emptyset) \tag{11}$$

Failure in compression occurs when maximum shear stress exceeds the formation cohesion and the frictional force. The straight line represents the failure envelope below which the formation is stable and above the line indicates borehole wall failure (Mitchell and Miska, 2011). The Mohr-Coulomb failure criterion is depicted in Figure 2. This criterion is used to analyse stress in this research project.

3. STRESS ANALYSIS

3.1 Wells at OW-731

TABLE 1: Orientations of wells at drill pad OW-731

Well	Trajectory	Inclination (°)	KOP (m)	Target direction	Elevation M.a.s.l.
OW-731	Vertical	0	0	Vertical	2215
OW-731A	Directional	20	500	N135°E	2215
OW-731B	Directional	20	400	N225°E	2220
OW-731C	Directional	20	400	N270°E	2220
OW-731D	Directional	20	400	N200°E	2221

The tectonic setting of Olkaria is in the continental East African Rift Valley dominated by normal faulting (Munyiri, 2016). Vertical stress σ_v form the maximum principal compressive stress with maximum (intermediate) horizontal stress σ_H parallel to the faulting direction (N-S) and the minimum horizontal stress σ_h perpendicular to faulting direction (Zoback, 2010). The wells orientations are shown in Table 2.

An average rock density of 2600 kg/m^3 (KenGen, 2017) is used to calculate the overburden stress at true vertical depths (TVD) to 3000 m which is then used together with pore pressure (BPD) with water table at 700 m and rock Poisson's Ratio (0.25) in the Eaton's Formula given by Equation 12 to calculate the minimum principal stress, pore pressure (BPD) and rock Poisson's Ratio (0.25) (Kearey et al., 2002; Fjær et al., 2008). Maximum horizontal stress is estimated as the average between vertical and minimum horizontal (Economides et al., 1998).

$$S_{hmin} = P_p + \frac{\vartheta}{1-\vartheta}\left(S_v - P_p\right) \quad (12)$$

Using the field stresses the effective stress variation calculated using effective stress Equations 3-8 depict how stress vary around the borehole wall. Points of high stress variation have high probabilities of failure.

3.2 Stress variation

Plotting effective hoop, radial and vertical stress around vertical wellbore wall indicates maximum compressive stress occurs at θ = 90° and 270° and minimum compressive stresses (tensile) occurs at θ = 0° and 180°. Radial stress from drilling fluid remains constant. Figure 3 show variation of stresses around vertical well OW-731 at 400 m.

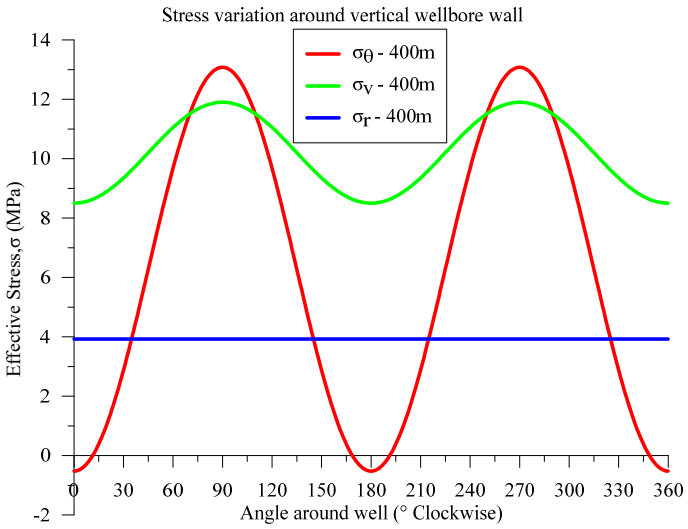

FIGURE 3: Effective stress variation around vertical wellbore at 400 m for OW-731

For directionally drilled wells, stress varies with the direction of the well in relation to the field stresses. Plotting effective hoop stress variation for directional wells at OW-731 shows how maximum and minimum stresses vary according to the well orientation. Radial stress remains constant around the wellbore and indicates the fluid pressure is the same around the wellbore. Variation of effective hoop stress at 750 m is depicted in Figure 4.

3.3 Wellbore stability

Assuming drilling fluid densities of 500 800, 1000, 1200 and 1800 kg/m^3, expressed in specific gravities (SG) of 0.5, 0.8, 1.0, 1.2 and 1.8 when divided with water density of 1000 kg/m^3, variations in effective stress with change in drilling fluid density are shown by Mohr's circles envelopes in vertical wellbore at 1000 m, and principal stresses at 791 m for directional well in Figure 5.

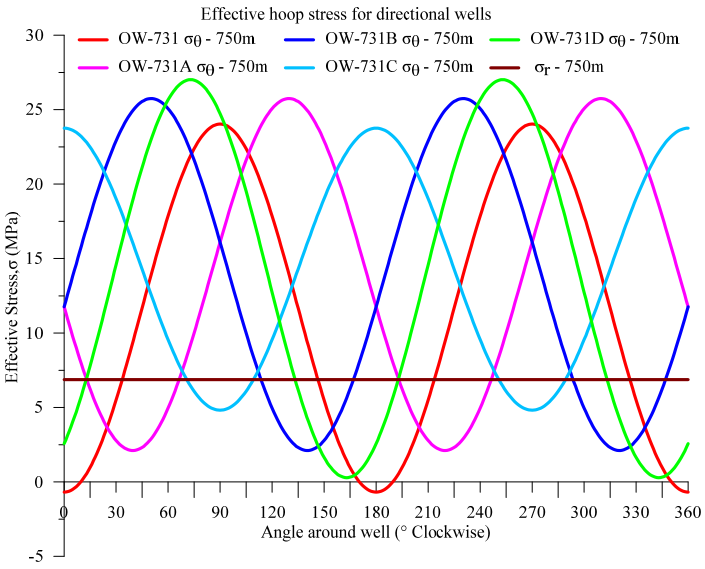

FIGURE 4: Effective hoop stress variation in directional wells at 750 m

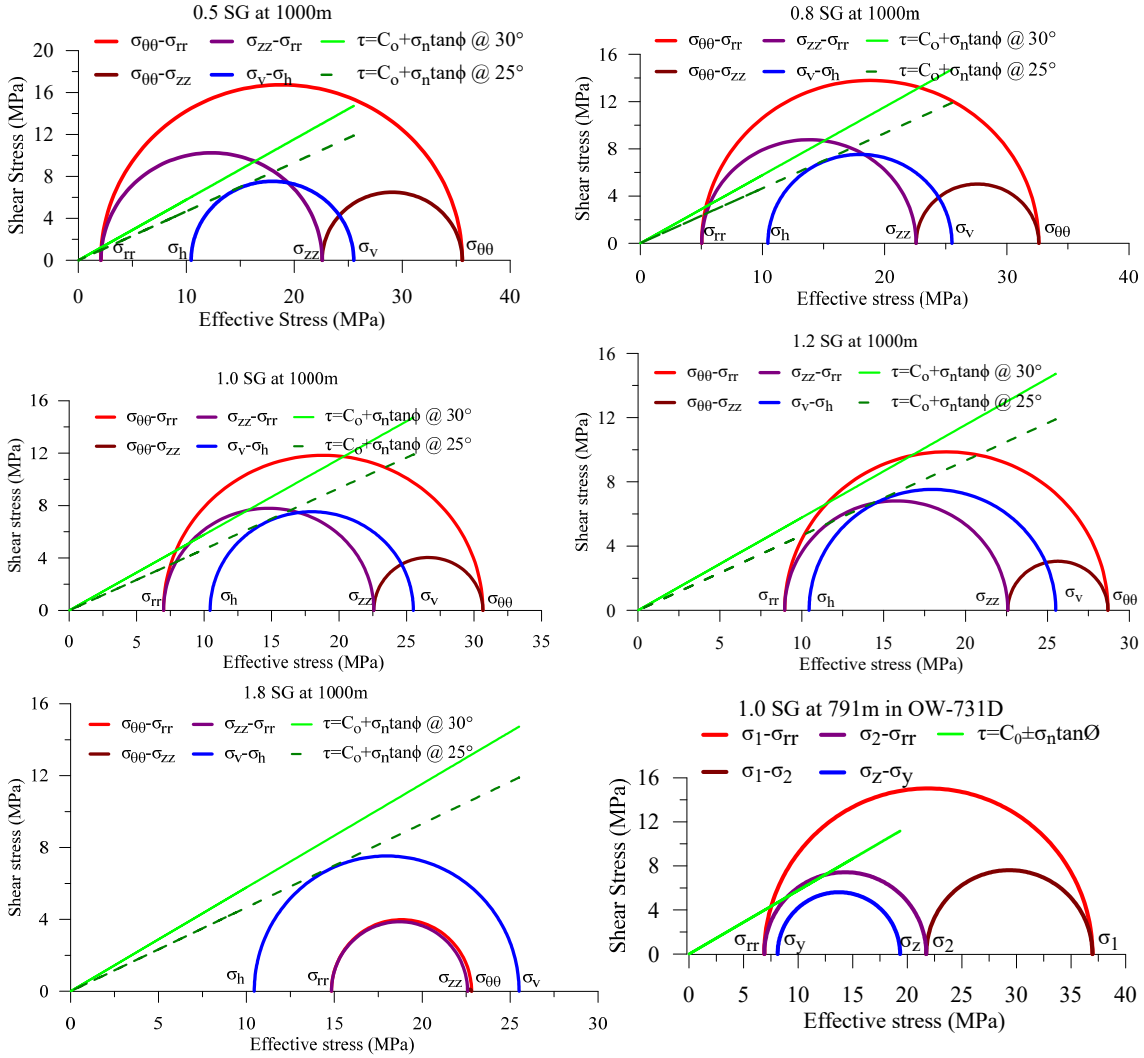

FIGURE 5: Failure envelops of effective stresses with drilling fluid density variation

4. CONCLUSIONS

Wellbore instability in wells caused by loss of circulation, wellbore collapse and creep are a result of induced stresses during drilling exceeding the borehole wall strength. Plotting Mohr´s circle diagrams (Figure 5) using maximum hoop stress, vertical stress and radial stress at different drilling fluid densities, indicate wellbore stability is improved with increase in drilling fluid density. Increase of drilling density reduces compressive hoop stresses that induce wellbore collapse but also increases possibility of formation fracture that results in loss of drilling fluid circulation. Mohr-Coulomb criteria for drilling fluid densities less than SG of 1.0 show the effective stresses plot above the failure line but below the line for 1.8 SG. This highlights the need to properly manage drilling fluid density during drilling.

The difference between radial and tangential effective stresses creates shear stresses that induce wellbore failure either through compressive collapse or tensile fracturing. Plotting stress variation around the wellbore indicates high compressive stresses at 90° and 270° and low stresses at 0° and 180° for vertical wells (Figure 3). In the directional wells (Figure 4), variation of the stresses is dependent on the inclination angle and azimuth. Comparing vertical and directional wells shows directional wells experience higher compressive stresses compared to vertical wells. This increases chances of having more instability concerns during drilling.

Managing wellbore instabilities during drilling requires extra material input than planned for and requires time, thereby slowing down drilling progress. Both time and material resources contribute to increase in the overall well cost.

ACKNOWLEDGEMENTS

I am grateful to the United Nations University Geothermal Training Program (UNU-GTP) for granting me this study opportunity and supporting my stay in Iceland.

REFERENCES

Aadnoy, B.S., and Looyeh, R., 2011: *Petroleum rock mechanics: drilling operations and well design.* Gulf Professional Publishing, 376 pp.

African Union, 2016: *The African Union Code of practice for geothermal drilling.* African Union Commission, Regional Geothermal Coordination Unit, Addis Ababa, Ethiopia.

Azar, J.J., and Samuel, R.G., 2007: *Drilling engineering.* PennWell Corporation, Tulsa, OK, 491 pp.

Economides, M.J., Watters, L.T., and Norman, S.D. 1998: *Petroleum well construction.* John Wiley & Sons Ltd., Chichester, West Sussex, 640 pp.

European Union, 2015: *2014 JRC geothermal energy status report.* Publications Office of the European Union, Joint Research Centre (JRC), Institute for Energy and Transport, Luxembourg.

Finger, J., and Blankenship, D., 2010: *Handbook of best practices for geothermal drilling.* Sandia National Laboratories, U.S. Department of Energy, Livermore, CA, 84 pp.

Fjær, E., Holt, R.M., Horsrud, P., Raaen, A.M., and Risnes, R., 2008: *Petroleum related rock mechanics* (2nd ed.). Elsevier, Amsterdam, The Netherland, 515 pp.

Harrison, J.P., and Hudson, J.A., 2000: *Engineering rock mechanics: part 2: Illustrative worked examples.*: Elseviewer Science, London, 530 pp.

Jaeger, J.C., Cook, N.G., and Zimmerman, R.W., 2007: *Fundamentals of rock mechanics.* Blackwell Publishing, USA, 475 pp.

Kearey, P., Brooks, M., and Hill, I., 2002: *An introduction to geophysical exploration* (3rd ed.). Blackwell Science Ltd., London, 262 pp.

KenGen, 2017: *Daily geological well logging report.* KenGen, Geology Section, Olkaria.

Mitchell, R.F., and Miska, S.Z., 2011: *Fundamentals of drilling engineering.* Society of Petroleum Engineers, SPE, Richardson, Texas, 696 pp.

Munyiri, S.K, 2016: *Structural mapping of Olkaria Domes geothermal field using geochemical soil gas surveys, remote sensing and GIS.* University of Iceland, MSc thesis, UNU-GTP, report 5, 100 pp.

Ouma, P., Koech, V., and Mwarania, F., 2016: Olkaria geothermal field reservoir response after 35 years of production (1981-2016). *Proceedings of the 6th African Rift Geothermal Conference - ARGeo-C6, Addis Ababa, Ethiopia,* 13 pp.

Rabia, H., 2001: *Well engineering and construction.* Entrac Consulting, 650 pp.

Renpu, W., 2011: *Advanced well completion engineering* (3rd ed.). Gulf Professional Publishing, Elsevier, Walthan, USA, 737 pp.

Zoback, M.D., 2010: *Reservoir geomechanics.* Cambridge University Press, NY, 461 pp.

Zoback, M.D., Barton, C.A., Brudy, M., Castillo, D.A., Finkbeiner, T., Grollimund, B.R., Moos, D.B., Peska, P., Ward, C.D., and Wiprut, D.J., 2003: Determination of stress orientation and magnitude in deep wells., *Internat. J. Rock Mechanics & Mining Sciences, 40,* 1049–1076.